Available online at www.sciencedirect.com
SCIENCE DIRECT
Biochemical and Biophysical Research Communications 344 (2006) 263–271
BBRC
www.elsevier.com/locate/ybbrc

Differential analysis of D-β-Asp-containing proteins found in normal and infrared irradiated rabbit lens

Takumi Takata [a], Tadashi Shimo-Oka [b], Masami Kojima [c], Kunio Miki [d], Noriko Fujii [a,*]

[a] Research Reactor Institute, Kyoto University, Kumatori-cho, Sennan, Osaka 590-0494, Japan
[b] Life Science Center, Asahi Techno Glass Corp, Funabashi, Chiba 273-0044, Japan
[c] Department of Ophthalmology, Kanazawa Medical University, Uchinada-cho, Kahoku, Ishiawa 920-0293, Japan
[d] Department of Chemistry, Kyoto University, Oiwake-cho, Kitashirakawa, Sakyo-ku, Kyoto 606-8502, Japan

Received 1 March 2006

Abstract

Although proteins are generally composed of L-α-amino acids, D-β-aspartic acid (Asp)-containing proteins have been reported in various elderly tissues. Our previous study detected several D-β-Asp-containing proteins in a rabbit lens derived from epithelial cell line by Western blot analysis of a 2D-gel using a polyclonal antibody that is highly specific for D-β-Asp-containing proteins. The identity of each spot was subsequently determined by matrix-assisted laser desorption/ionization time-of-flight mass spectrometry and the Ms-Fit online database searching algorithm. In this study, we discovered novel D-β-Asp-containing proteins from rabbit lens. The results indicate that β-crystallin A3, β-crystallin A4, β-crystallin B1, β-crystallin B2, β-crystallin B3, γ-crystallin C, γ-crystallin D, and λ-crystallin in rabbit lens contain D-β-Asp residues. Furthermore, the occurrence of D-β-Asp residues increases with infrared ray (IR) irradiation. Additionally, some D-β-Asp-containing proteins only appear after IR irradiation. One such protein is the α-enolase, which shows homology to τ-crystallin.

Keywords: β-Crystallin; γ-Crystallin; λ-Crystallin; α-Enolase; Lens; Two-dimensional electrophoresis; D-Amino acid; Posttranslational modification; Proteomics; Infrared ray

Although proteins consist exclusively of L-amino acids, D-aspartic acid (D-Asp) has been detected in various tissues such as tooth [1], bone [2], aorta [3], brain [4], erythrocyte [5], eye lens [6], skin [7], and lung [8] from elderly individuals. The presence of D-Asp in aged tissues of living organisms is thought to result from the racemization of aspartyl residues in the polypeptide of proteins derived from metabolically inert tissues. We previously reported the presence of D-isomers at Asp-58 and Asp-151 in αA-crystallin [9,10], and at Asp-36 and Asp-62 in αB-crystallin [11] from aged human lenses. D-Asp formation was accompanied by isomerization from the natural α-Asp to the abnormal β-Asp [12]. Therefore, the normal L-α-Asp converts to L-β-Asp, D-α-Asp, and D-β-Asp via a five-membered succinimide intermediate in the protein. Among these uncommon isomers, D-β-Asp was the major isomer found in elderly tissues [13]. Racemization and isomerization of amino acids in protein can cause major changes to the 3D-structure because different side chain orientations can induce an abnormal peptide backbone. Therefore, these posttranslational modifications may induce the partial unfolding of protein leading to a disease state. Although the study of the racemization of Asp in proteins has been mainly limited to aged tissues, biochemical analysis shows that the formation of D-β-aspartic acid at Asp-151 of human αA-crystallin occurs even in newborn human lenses [9]. Recently, we identified many D-β-Asp-containing proteins from the actively dividing N/N1003A cell line, which is commonly used in lens research [14]. The results suggest that D-β-aspartic acid formation may occur at the early stage of differentiation in the lens epithelium.

* Corresponding author. Fax: +81 724 51 2496.
E-mail address: nfujii@HL.rri.kyoto-u.ac.jp (N. Fujii).

0006-291X/$ - see front matter © 2006 Elsevier Inc. All rights reserved.
doi:10.1016/j.bbrc.2006.03.126

We have determined the activation energy for the racemization of the Asp151 residue using a model peptide corresponding to a portion of human αA-crystallin [15]. The activation energy for Asp racemization and isomerization in the model peptide was ~20 kcal/mol. Intriguingly, this value corresponds to the energy of IR. Here, we report the detection of D-β-Asp-containing proteins in rabbit lens that have been exposed to IR. A combination of 2D-PAGE, MALDI-TOF-MS analysis, computer searching algorithm, and an online protein database were used to identify the modified proteins. We observed an increase of D-β-Asp-containing proteins in rabbit lens as a result of exposure to IR. Our findings indicate that the inversion and isomerization of an Asp-residue is increased by IR irradiation. Specifically, we report the presence of D-β-Asp-containing β-, γ-, and λ-crystallins in both irradiated and non-irradiated rabbit lens. Furthermore, D-β-Asp-containing α-enolase was detected exclusively in IR irradiated lens.

Materials and methods

Materials. Thirty-week-old rabbits (Dutch kind) were prepared in specific-pathogen-free conditions. The rabbit lens from one eye of each rabbit was irradiated using a laser diode (1260 nm) at 162 J for 30 min before being excised and stored. The opposite non-irradiated eye of the same rabbit was used as a control non-irradiated lens. Lenses were thawed on ice and then homogenized (2 ml/lens) in buffer (50 mM Tris–HCl, pH 7.9, containing protease inhibitor cocktail (SIGMA, Tokyo, Japan)). The lens homogenate was clarified by centrifugation (15,000*g* for 15 min) and the supernatant was pooled and re-suspended in extraction buffer (8 M urea, 2 M thiourea, 4% 3-[(3-cholamidopropyl) dimethylammonio]-1-propanesulfonate (Chaps), and 65 mM dithiothreitol (DTT)) on ice. The cell-free extract was clarified by centrifugation (15,000*g*, 15 min) and the supernatant was collected. Finally, a 2% immobilized pH gradient (IPG) buffer and a trace of bromophenol blue were added to the supernatant. Total protein concentration was determined using the Bradford assay [16]. Each preparation was subjected to two-dimensional gel electrophoresis: isoelectric focusing (IEF) in the first dimension and SDS–PAGE in the second dimension. The IEF separation was carried out using Immobiline Dry Strips (18 cm, pH 3–10) by following the manufacturer's suggested method (Amersham Biosciences, Piscataway, NJ). Prior to the first IEF analysis, the supernatant was incubated overnight with dry strips at 4 °C. IEF analysis was performed using an EPS 3501XL power supply (Amersham Biosciences) for 18 h at 15 °C. After IEF, the IPG strips were equilibrated for 20 min in equilibration buffer (50 mM Tris–HCl, pH 6.8, containing 6 M urea, 2% SDS, 30% glycerol, and 200 mM DTT). Strips were then re-equilibrated for 20 min in the same buffer containing 135 mM iodoacetamide instead of DTT. In all cases, molecular weight separation was achieved using an ExcelGel SDS XL gradient 12–14 (Amersham Biosciences). The protein spots on the gel were visualized by staining with Coomassie blue.

Antibodies and ELISA. The following antibodies were used in this study: anti-peptide 3R antibody, which was prepared as described previously [17]. This rabbit antibody is highly specific against Gly-Leu-D-β-Asp-Ala-Thr-Gly-Leu-D-β-Asp-Ala-Thr-Gly-Leu-D-β-Asp-Ala-Thr that corresponds to three repeats of positions 149–153 in human αA-crystallin. For the ELISA, polystyrene microtiter ELISA plates (Asahi Techno Glass, Funabashi, Japan) were used. Each well was coated with 50 μl of respective antigen (1 mg/ml) in PBS at 4 °C overnight. As a blank, some wells were coated with PBS only. The plates were washed twice with washing buffer (Asahi Techno Glass) and coated with PBS containing 10 mg/ml BSA for 60 min at 25 °C. This was followed by at diluted 10-, 100-, 1000- or 10,000-fold, to the wells and incubated for 60 min at 25 °C. Unbound antibodies were removed from the plates by washing them five times in washing buffer. Bound antibodies were reacted with a goat anti-rabbit immunoglobulin coupled with horseradish peroxidase for 60 min at 25 °C. After five washing cycles using the buffer, the bound enzymatic activity was measured by 3,3′,5,5′-tetramethylbenzidine as a substrate. Duplicate determinations were performed for each assay. In the previous study, we also synthesized the peptide IQTGLDATHAER, corresponding to the amino acid sequences 146–157 in human αA-crystallin in which Asp residues were normal L-α-Asp, abnormal D-α-Asp, L-β-Asp or D-β-Asp. Specifically: (1) Ile-Gln-Thr-Gly-Leu-L-α-Asp-Ala-Thr-His-Ala-Glu-Arg. (2) Ile-Gln-Thr-Gly-Leu-L-β-Asp-Ala-Thr-His-Ala-Glu-Arg. (3) Ile-Gln-Thr-Gly-Leu-D-α-Asp-Ala-Thr-His-Ala-Glu-Arg. (4) Ile-Gln-Thr-Gly-Leu-D-β-Asp-Ala-Thr-His-Ala-Glu-Arg. The anti-peptide 3R antibody was clearly distinguished between the configuration of the Asp-residue because it reacted very strongly with the D-β-Asp-containing peptide but not with the L-α-Asp, L-β-Asp, and D-α-Asp-containing peptides [17,18].

We used a goat anti-rabbit IgG conjugated to horseradish peroxidase (HRP) as the second antibody (MP Biomedicals, Aurora, OH).

Western blot. For Western blot analysis, extracted proteins from the lens were separated by 2D-PAGE and then transferred to Immobilon TM transfer PVDF membrane (0.45 μm) (Millipore, Bedford, MA). The membrane was blocked with 5% non-fat milk, 0.1% BSA in 0.1% polyoxyethylene sorbitan monolaurate (Tween 20) containing Tris-buffered saline (TBS) overnight at 4 °C. The membrane was washed three times with TBS containing 0.1% Tween 20 and then incubated for 1 h at room temperature with the first antibody (1:250). After three washes with TBS containing 0.1% Tween 20, the membrane was incubated for 1 h at room temperature with horseradish peroxidase-conjugated secondary antibody (1:500). Following another three washes with TBS containing 0.1% Tween 20, labeled proteins were visualized using enhanced chemiluminescence (ECL Plus Western blotting detection kit, Amersham Bioscience) on BioMax MS film (Kodak, Rochester, NY).

Image analysis. The density of each spot from irradiated samples was compared to non-irradiated samples on Western blotting membrane. All the differentially expressed proteins detected by Western blotting were excised after staining two-dimensional gels with Coomassie brilliant blue G-250 (CBB) for MALDI-TOF-MS analysis.

In-gel digestion. Enzyme digestion of proteins in the CBB stained gel was performed as follows: protein spots excised from the CBB stained gel were de-stained with 50% MeOH/50 mM ammonium bicarbonate and cut into 1–2 mm slices using a spot cutter. The gel pieces were then washed with 50% acetonitrile/50 mM ammonium bicarbonate and incubated with acetonitrile. The gel pieces were dried in a SpeedVac vacuum concentrator and then re-hydrated using 25 μl of trypsin solution (Promega, Madison, WI). Digestion was continued at 37 °C for 12 h. The tryptic peptides were first extracted using 0.1% TFA/50% acetonitrile and then re-extracted twice using the same solution after 15 min agitation. The extracted samples were mixed in an Eppendorf tube and then dried in a vacuum concentrator prior to MALDI-TOF-MS analysis.

Identification of D-β-Asp-containing proteins by MALDI-TOF-MS. All MALDI-TOF-MS experiments were performed using a Voyager DE Pro (Applied Biosystems, Foster City, CA) instrument. The matrix (α-cyano-4-hydroxycinamic acid) was made up to a saturated solution with 0.1% trifluoroacetic acid/70% acetonitrile. The sample solution and the matrix solution were mixed and applied in a 100-well target using Zip-Tip c-μ18 (Millipore) and air-dried. External calibration was achieved with a peptide mixture provided by ABI. Protein identification was conducted using Ms-Fit software (available on the internet) against the Swiss-Plot Database.

Results

Infrared irradiation of rabbit lens

A previous study determined the activation energy for the racemization of Asp in a human lens model peptide

to be 20–30 kcal/mol [15]. This energy level corresponds to the wavelength region of IR. Therefore, we irradiated rabbit lens with IR radiation using a laser diode (1260 nm) at 162 J for 30 min (equivalent to 20–30 kcal/mol). No apparent morphological or pathological changes were detected in the rabbit eyes 1 month after irradiation.

Investigation of D-β-Asp-containing lens soluble fraction

ELISA was carried out to evaluate the specificity and titer of the anti-peptide 3R antibody. The results are shown in Fig. 1. The antibody reacted most strongly with human α-crystallin obtained from elderly donors (80-year-old subjects). The antibody also reacted with aged bovine α-crystallin and soluble fractions of rabbit lens, but the reactivity to recombinant αA-crystallin was negligible. Fig. 1 indicates that the antibody specifically recognizes the D-β-Asp-containing peptide in the soluble fraction of non-irradiated rabbit lens as well as human and bovine α-crystallin. Our previous study also suggests that the antibody reacts very strongly with the D-β-Asp T18 peptide but not with the L-α-Asp T18, L-β-Asp T18, and D-α-Asp T18 peptides despite having the same sequence [17].

Detection of D-β-Asp containing proteins by 2D-electrophoresis

D-β-Asp-containing proteins were detected in the soluble fraction of the rabbit lens following extraction, separation by 2D-gel electrophoresis, and analysis by Western blotting using the anti D-β-Asp-containing peptide antibody. Fig. 2 shows the Western blotting of the lens soluble fraction from IR irradiated and non-irradiated rabbit lenses. A significantly greater level of D-β-Asp immune reactivity was present in the lens subjected to IR irradiation. Fig. 3 shows the CBB stained 2D-electrophoresis gel map of the non-irradiated rabbit lens soluble fraction. The distribution of proteins derived from non-irradiated and IR irradiated lens was essentially identical (data not shown). The arrows in Fig. 3 indicate 20 D-β-Asp-containing proteins whose reactivity is significantly increased upon IR irradiation of the rabbit lens. In addition, three more D-β-Asp-containing proteins (spot Nos. 21–23) are found exclusively in IR irradiated lens (Fig. 2B).

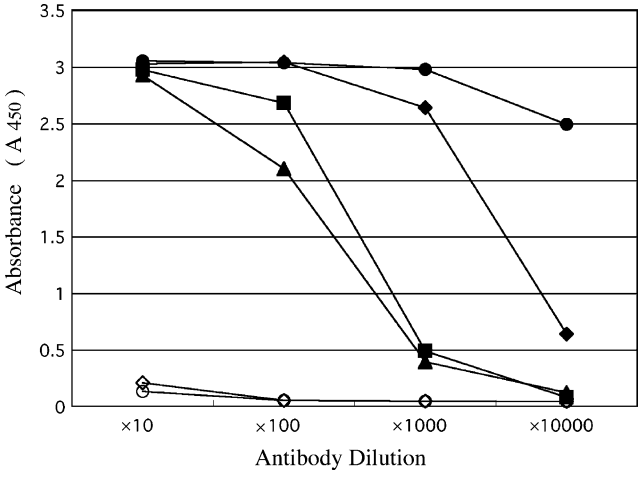

Fig. 1. Results of ELISAs for determining the specificity of antibody to many species of lens soluble fractions. The original antibody stock solution ($A_{280} = 0.301$) was diluted with 10 mg/ml BSA in PBS. Microtiter wells were coated with antigen (filled circle), α-crystallin derived from aged human (filled diamond), aged bovine (filled square), rabbit (filled triangle) lenses, and recombinant αA-crystallin (open circle). Blank wells were not coated with αA-crystallin (open diamond).

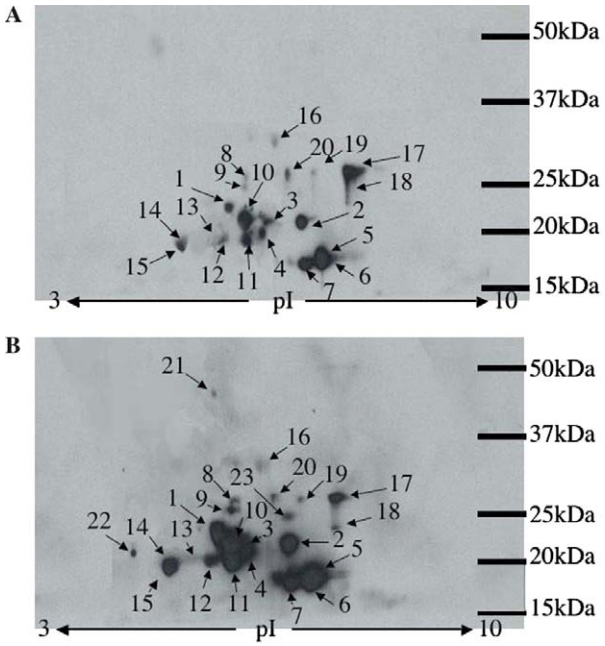

Fig. 2. Two-dimensional gel electrophoretic separation of proteins derived from infrared irradiated and non-irradiated rabbit lens, and identification of D-β-Asp containing proteins in the pH 3–10 range. (A) Western blotting of the non-irradiated rabbit lens soluble fraction with anti-peptide 3R antibody. SDS–PAGE using a linear 12–14% gradient gel performed at pH 3–10. Arrows indicate D-β-Asp-containing proteins. (B) Western blotting of the infrared irradiated rabbit lens soluble fraction probed with anti-peptide 3R antibody. SDS–PAGE using a linear 12–14% gradient gel performed at pH 3–10. Arrows indicate D-β-Asp-containing proteins.

Identification of D-β-Asp-containing proteins by MALDI-TOF-MS analysis

Proteins detected by immunostaining on the 2D-gel were analyzed by subjecting the corresponding CBB-stained protein to mass spectrometry. We selected 23 spots (indicated by arrows in Fig. 3) from the 2D-gel, which were tentatively identified as D-β-Asp-containing proteins, for in-gel trypsinization and analysis by MALDI-TOF-MS. The mass data were fitted by MS-Fit using the Swiss-Prot database search analysis. Because some of the lens proteins run as multiple spots by 2D-gel electrophoresis, 9 proteins were identified from 23 spots (Table 1). One typical mass spectrum from this series of experiments is shown in Fig. 4 (i.e., spot No. 1). As shown in Table 1, spot numbers 1, 2, 3, 4, and 18 were identified as β-crystallin B3. Five strong

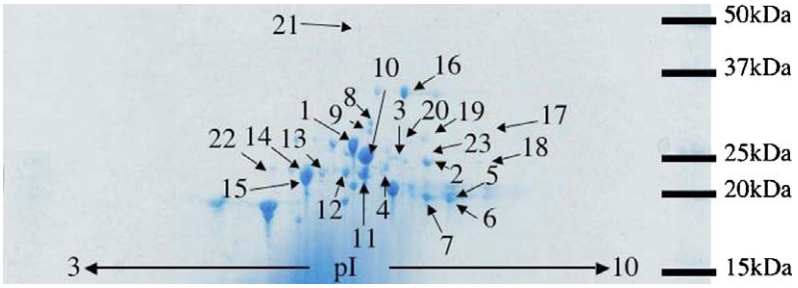

Fig. 3. Two-dimensional gel electrophoretic separation of proteins derived from non-irradiated rabbit lens soluble fraction. 2D Coomassie brilliant blue stained gel map of the rabbit lens soluble fraction. Spots that were detected by immunoblot analysis are indicated by arrows and numbered from 1 to 23 on the 2D gel image. Numbered spots were excised and analyzed by in-gel trypsin digestion and MALDI-TOF-MASS spectrometry. Numbers shown here are the same as Fig. 2 and are listed in Table 1.

signals (*m*/*z* 1729.38, 1774.47, 2008.48, 2230.54, and 2358.62), matching the predicted mass values of β-crystallin B3 in the Swiss-Prot database, were detected (shown in Table 1). The average mass accuracy for all peaks was 300 ppm. Total coverage represented 39% of the predicted protein sequence. Several other spots that showed reactivity against the antibody were also identified by this analysis. These spots were identified as β-crystallin A3 (spot No. 12), β-crystallin A4 (spot Nos. 13–15), β-crystallin B1 (spot Nos. 8–9, 17), β-crystallin B2 (spot Nos. 10–12), β-crystallin B3, γ-crystallin C (spot Nos. 6–7), γ-crystallin D (spot No. 5), and λ-crystallin (spot No. 16) in non-irradiated rabbit lens. The main peaks, average mass accuracy and total coverage for the predicted protein sequence for each spot are summarized in Table 1.

Discussion

Our previous studies showed that stereoinversion and isomerization occurs at Asp-151 and Asp-58 in αA-crystallin from aged human lens tissues, forming L-β, D-α, and D-β-isomers. We reported the activation energy for the racemization of the Asp151 residue in a human αA-crystallin model peptide to be about 20–30 kcal/mol in kinetic measurements [15]. The accumulation of these abnormal isomers of Asp residues may lead to a distortion in the higher order structure of αA-crystallin. The formation of the isomers begins shortly after birth and continues throughout the aging process.

In this study, we used MALDI-TOF-MS analysis to detect some D-β-Asp-containing proteins from non-irradiated rabbit lens. Among the 23 gel spots, 20 were identified by MALDI-TOF-MS. The failure to identify all the protein spots is probably due to a number of different factors. First, some of the gel bands appear diffused due to the presence of elution salts, which might decrease the digestion efficiency and/or recovery of the peptides. This is particularly important for minor spots where MALDI-TOF-MS failed to identify any protein signals as a result of poor resolution and/or mass inaccuracy. Alternatively, the spot may represent an unknown protein, which is often difficult to resolve by MALDI-TOF-MS. Because the rabbit database is incomplete, we assumed that the distribution of rabbit crystallins is similar to that of other mammals. The high degree of homology shared among the crystallins from various species allowed us to identify D-β-Asp-containing β-, γ-crystallin, and λ-crystallin. The latter protein is rabbit specific. The level of each representative D-β-Asp-containing protein increased dramatically after exposure of the lens to IR irradiation. Furthermore, a few of the D-β-Asp-containing proteins were only found in rabbit lens exposed to IR. Interestingly, we did not observe D-β-Asp-containing α-crystallin in either unexposed or IR exposed lenses. In this study, we demonstrate that most rabbit crystallins contain D-β-Asp residues. The racemization/isomerization of Asp in β-, γ- and λ-crystallin has never been reported in mammals. β-Crystallins are major protein constituents of the mammalian lens, where their stability and association into higher order complexes is critical for lens clarity and refraction. There are many kinds of β-crystallins in mammalian lens. β-Crystallin has high homology with γ-crystallin. γ-Crystallin contains many components (γ A–γ F). Together with the α A- and β-crystallins, these proteins are essential for maintaining lens transparency. γ-Crystallin is a monomer that is synthesized in the early stages of development and is abundant in the nucleus. Unlike α-crystallin, the three-dimensional structure has been reported with many γ-crystallins [19].

Our study has established that D-β-Asp-containing β-, γ-, and λ-crystallins are present in non-irradiated rabbit lens. Interestingly, β- and γ-crystallins are highly conserved, having a common polypeptide chain fold, and constitute a superfamily of β-, γ-crystallins [20] characterized by the Greek key motif [21]. Mutations in β, γ-crystallin genes at the Greek key motif can lead to nonspecific aggregation of crystallins resulting in cataract formation. In addition, many mutations in the Greek key motif that alter γ-crystallin association also cause cataracts. Some site-specific mutations have been reported in many cataract lenses [20,22–24]. Indeed, these mutations may be responsible for the solubility of lens crystallins and lens transparency. Racemization and isomerization of Asp is induced by changes in the common motif in β- and γ-crystallins. Alternatively, these mutations result in an altered 3D structure with aging.

Table 1
List of proteins displaying reactivity against the anti-D-β-Asp antibody

Spot No. 1									
m/z	1729.83			1774.91		2007.94	2230.02		2358.12
M_w (mono)	1729.38			1774.47		2008.48	2230.54		2358.62
Delta (Da)	0.45			0.44		−0.54	−0.52		−0.50
Modification									
Position	153–167			56–71		180–195	129–147		128–147
Identified protein	Average mass accuracy (ppm)			Accession No.		M_w (Da)	Coverage (%)		Score
β-Crystallin B3	300			P19141		24328	39		2146
Spot No. 2									
m/z	1323.71			1387.71		1757.87	1774.91		2007.94
M_w (mono)	1323.58			1387.57		1757.70	1774.76		2007.83
Delta (Da)	0.13			0.14		0.17	0.16		0.11
Modification									
Position	73–83			116–127		153–167	56–71		180–195
Identified protein	Average mass accuracy (ppm)			Accession No.		M_w (Da)	Coverage (%)		Score
β-Crystallin B3	300			P02524		24276	33		1386
Spot No. 3									
m/z	1323.71			1387.71		1757.87	1774.91		2007.94
M_w (mono)	1323.58			1387.57		1757.70	1774.76		2007.83
Delta (Da)	0.13			0.14		0.17	0.16		0.11
Modification									
Position	73–83			116–127		153–167	56–71		180–195
Identified protein	Average mass accuracy (ppm)			Accession No.		M_w (Da)	Coverage (%)		Score
β-Crystallin B3	300			P02524		24276	33		771
Spot No. 4									
m/z	1323.71	1387.71	1537.77	1774.91	1931.01	2007.94	2230.02	2246.02	2358.12
M_w (mono)	1323.69	1387.69	1537.73	1774.90	1931.04	2007.96	2230.05	2245.98	2358.13
Delta (Da)	0.02	0.02	0.03	0.01	−0.03	−0.02	−0.02	0.04	−0.01
Modification								1MetOX	
Position	73–83	116–127	76–88	56–71	56–72	180–195	129–147	129–147	128–147
Identified protein	Average mass accuracy (ppm)			Accession No.		M_w (Da)	Coverage (%)		Score
β-Crystallin B3	300			Q9JJU9		24291	38		7.07E+04
Spot No. 5									
m/z	943.45	1277.66	1294.69	1348.62	1450.79	2199.99	2736.26		
M_w (mono)	943.57	1277.79	1294.82	1348.83	1450.87	2200.16	2736.27		
Delta (Da)	−0.12	−0.13	−0.13	−0.21	−0.08	−0.17	−0.01		
Modification		pyro Glu							
Position	4–10	143–152	143–152	153–163	143–153	60–70	38–59		
Identified protein	Average mass accuracy (ppm)			Accession No.		M_w (Da)	Coverage (%)		Score
γ-Crystallin D	100			P08209		20867	39		3982
Spot No. 6									
m/z	943.45	1348.70	1365.73	2044.91	2201.01	2217.00	2248.12	2806.31	
M_w (mono)	943.56	1348.81	1365.85	2045.03	2201.19	2217.18	2248.31	2806.15	
Delta (Da)	−0.11	−0.11	−0.12	−0.12	−0.18	−0.17	−0.19	0.16	
Modification		pyro Glu				1MetOX		1MetOX	
Position	4–10	143–152	143–152	61–77	60–77	60–77	123–140	38–59	
Identified protein	Average mass accuracy (ppm)			Accession No.		M_w (Da)	Coverage (%)		Score
γ-Crystallin C	100			P07315		20879	43		5.51E+04
Spot No. 7									
m/z	943.45	1365.73	2217.00	2638.20	2790.31	2795.28	2806.31		
M_w (mono)	943.55	1365.83	2217.17	2638.55	2789.55	2794.52	2807.05		
Delta (Da)	−0.10	−0.10	−0.17	−0.35	0.76	0.76	−0.74		
Modification			1MetOX			2MetOX	1MetOX		
Position	4–10	143–152	60–77	11–32	38–59	100–122	38–59		
Identified protein	Average mass accuracy (ppm)			Accession No.		M_w (Da)	Coverage (%)		Score
γ-Crystallin C	300			P07315		20879	58		2.58E+04

(*continued on next page*)

Table 1 (*continued*)

Spot No. 8					
m/z	1457.71	1465.74	1621.85	1970.90	2631.15
M_w (mono)	1457.71	1465.75	1621.79	1970.93	2631.23
Delta (Da)	−0.01	−0.01	0.05	−0.03	−0.08
Modification					
Position	201–212	59–70	59–71	72–88	159–180
Identified protein	Average mass accuracy (ppm)	Accession No.	M_w (Da)	Coverage (%)	Score
β-Crystallin B1	100	P02523	28093	25	478
Spot No. 9					
m/z	1457.71	1465.74	1970.90		2631.15
M_w (mono)	1457.69	1465.73	1970.89		2631.15
Delta (Da)	0.01	0.01	0.01		0.00
Modification					
Position	201–212	59–70	72–88		159–180
Identified protein	Average mass accuracy (ppm)	Accession No.	M_w (Da)	Coverage (%)	Score
β-Crystallin B1	100	P02523	28093	25	327
Spot No. 10					
m/z	1024.45	1269.63	1585.77	1760.84	2190.02
M_w (mono)	1024.46	1269.64	1585.76	1760.90	2190.11
Delta (Da)	−0.01	−0.01	0.01	−0.06	−0.09
Modification					
Position	82–89	190–198	69–81	146–160	169–188
Identified protein	Average mass accuracy (ppm)	Accession No.	M_w (Da)	Coverage (%)	Score
β-Crystallin B2	50	P43320	23380	31	78.8
Spot No. 11					
m/z	1024.45	1760.84	2190.02		2759.31
M_w (mono)	1024.16	1760.30	2189.43		2759.48
Delta (Da)	0.29	0.54	0.59		−0.17
Modification					
Position	82–89	146–160	169–188		122–145
Identified protein	Average mass accuracy (ppm)	Accession No.	M_w (Da)	Coverage (%)	Score
β-Crystallin B2	50	P43320	23380	32	209
Spot No. 12					
m/z	1466.80	1611.81	1691.76	1727.85	1920.85	2434.08
M_w (mono)	1466.38	1611.35	1691.28	1727.35	1920.32	2433.41
Delta (Da)	0.42	0.46	0.48	0.49	0.53	0.67
Modification						
Position	126–137	33–45	96–109	197–211	163–177	178–196
Identified protein	Average mass accuracy (ppm)	Accession No.	M_w (Da)	Coverage (%)	Score
β-Crystallin A3	300	P11843	25131	40	658
Spot No. 13					
m/z	1466.76	1773.87	2172.93		2578.28
M_w (mono)	1466.44	1773.44	2172.41		2577.72
Delta (Da)	0.33	0.43	0.52		0.56
Modification					
Position	121–132	192–206	86–104		63–85
Identified protein	Average mass accuracy (ppm)	Accession No.	Mw (Da)	Coverage (%)	Score
β-Crystallin A4	300	P11842	23861	32	1100
Spot No. 14							
m/z	1773.87	1954.84	2172.93	2221.06	2377.16	2395.07	2578.28
M_w (mono)	1773.37	1954.31	2172.33	2220.49	2376.54	2394.43	2577.63
Delta (Da)	0.50	0.53	0.60	0.57	0.62	0.64	0.65
Modification							
Position	192–206	173–188	86–104	41–59	40–59	173–191	63–85
Identified protein	Average mass accuracy (ppm)	Accession No.	M_w (Da)	Coverage (%)	Score
β-Crystallin A4	300	P11842	23861	45	7.00E+04

Table 1 (*continued*)

Spot No. 15										
m/z				1733.87			2377.16			2578.28
M_w (mono)				1773.61			2376.81			2577.85
Delta (Da)				−39.74			0.35			0.43
Modification										
Position				192–206			40–59			63–85
Identified protein	Average mass accuracy (ppm)			Accession No.		M_w (Da)		Coverage (%)		Score
β-Crystallin A4	300			P11842		23861		27		133
Spot No. 16										
m/z	905.47	1062.56	1114.62	1329.64	1345.64	1349.72	1680.93	2432.21		
M_w (mono)	905.64	1062.71	1114.77	1329.78	1345.79	1349.86	1681.03	2432.24		
Delta (Da)	−0.17	−0.15	−0.15	−0.14	−0.15	−0.13	−0.10	−0.04		
Modification					1MetOX		AcetN			
Position	34–40	189–197	41–50	20–31	20–31	198–208	1–19	209–231		
Identified protein	Average mass accuracy (ppm)			Accession No.		M_w (Da)		Coverage (%)		Score
λ-Crystallin	200			P14755		35273		28		3.80E+04
Spot No. 17										
m/z		1457.71		1465.74		2037.95		2038.04		
M_w (mono)		1457.57		1465.60		2037.69		2037.69		
Delta (Da)		0.14		0.15		0.27		0.35		
Modification										
Position		204–215		62–73		145–161		94–111		
Identified protein	Average mass accuracy (ppm)			Accession No.		M_w (Da)		Coverage (%)		Score
β-Crystallin B1	100			P07318		28144		23		133
Spot No. 18										
m/z	1323.71	1387.71	1757.87	1774.91	2007.94	2230.02	2358.12			
M_w (mono)	1323.49	1387.50	1757.60	1774.63	2007.64	2229.72	2357.80			
Delta (Da)	0.21	0.21	0.26	0.28	0.30	0.31	0.32			
Modification										
Position	73–83	116–127	153–167	56–71	180–195	129–147	128–147			
Identified protein	Average mass accuracy (ppm)			Accession No.		M_w (Da)		Coverage (%)		Score
β-Crystallin B3	300			P02524		24276		42		3.50E+05
Spot No. 19										
m/z	1187.51	1457.71	1465.74	2037.95	2038.04	2631.15				
M_w (mono)	1187.58	1457.78	1465.82	2038.15	2038.15	2631.31				
Delta (Da)	−0.07	−0.08	−0.07	−0.20	−0.11	−0.16				
Modification										
Position	125–133	204–215	62–73	145–161	94–111	162–183				
Identified protein	Average mass accuracy (ppm)			Accession No.		M_w (Da)		Coverage (%)		Score
β-Crystallin B1	100			P07318		28144		35		2416
Spot No. 20										
No matching										
Spot No. 21										
m/z	1007.50	1143.62	1495.71	1541.76	1556.78	1557.76	1633.82	1691.90	1804.94	1910.98
M_w (mono)	1007.44	1143.49	1495.97	1541.61	1556.61	1557.59	1633.66	1691.59	1804.75	1910.80
Delta (Da)	0.06	0.12	−0.26	0.16	0.17	0.17	0.16	0.31	0.19	0.18
Modification						1MetOX				
Position	336–343	184–193	93–105	359–372	240–253	359–372	344–358	407–420	33–50	163–179
Identified protein	Average mass accuracy (ppm)			Accession No.		M_w (Da)		Coverage (%)		Score
α-Enolase	200			P51913		47305		38		1.93E+06
Spot No. 22										
No matching										
Spot No. 23										
No matching										

Identification of D-β-Asp-containing proteins from the rabbit lens (Fig. 3) by screening with an anti-D-β-Asp antibody followed by tryptic peptide fingerprint mass spectrometry. Spot number indicates the protein spot in the 2D gel. Theoretical mass values, *m/z*; experiment *m/z* values (monoisotopic mass values), M_w (mono); molecular masses calculated from the matched proteins, Delta; Oxidation of methionine is abbreviated 1MetOX and 2MetOX; pyro-glutamic acid, pyroGlu; acetylation of N-terminal, AcetN. Accession number in Swiss-Prot databases. Theoretical M_w (Da). Sequence coverage % (MS data), and mouse score.

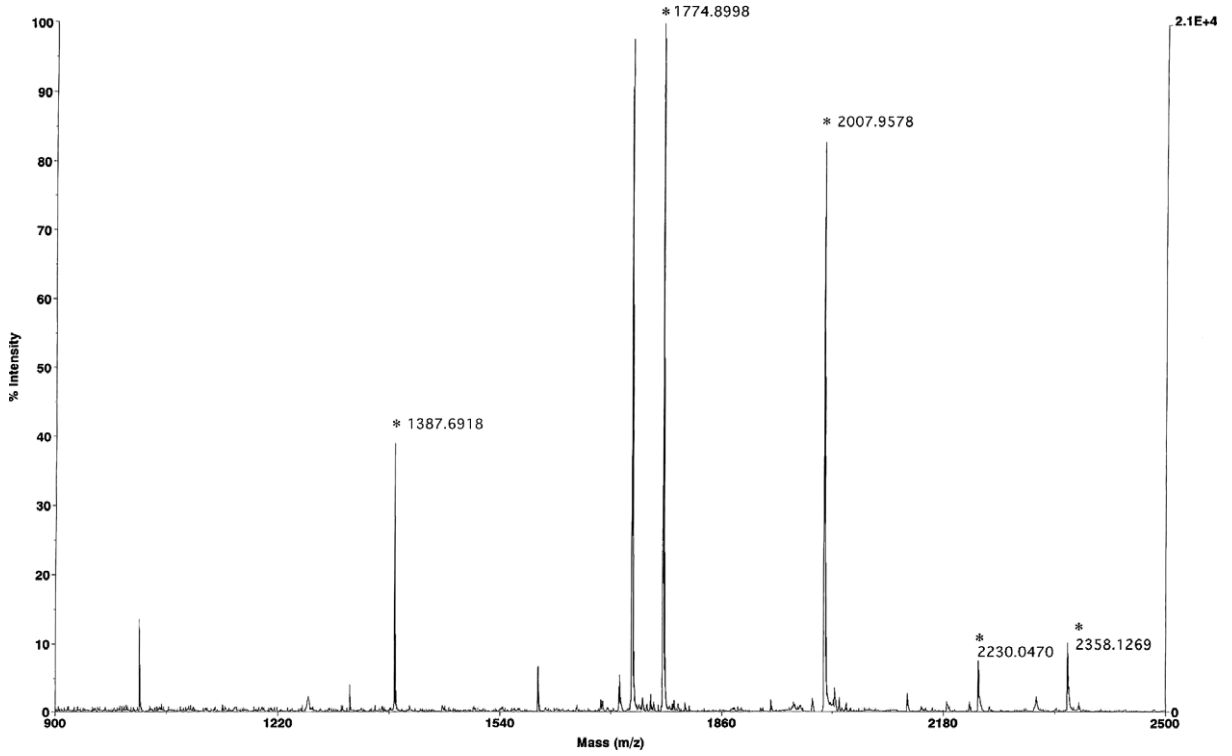

Fig. 4. Peptide map of spot No. 1 from the gel in Fig. 3. Peaks were sequenced and used for a database search. These peaks correspond to the tryptic digestion pattern of β-crystallin B3 (see Table 1).

This study has demonstrated that the level of D-β-Asp-containing protein markedly increases in the lens after IR irradiation (Fig. 2B). We believe IR stress, as much as the activation energy for the racemization reaction, promotes the racemization/isomerization of aspartic acid residues in proteins. The accumulation of D-β-Asp-containing polypeptides induces changes in the higher order structure of proteins. The Greek motif may be an important site for racemization and isomerization. The resultant disruption of the higher crystallin structures may be a major cause of increased opacity of the lens following exposure to IR. Further studies into the formation of D-β-Asp-containing proteins are required.

Interestingly, D-β-Asp-containing α-crystallin was not detected in either the non-irradiated or irradiated rabbit lens. λ-Crystallin, which is rabbit specific, has 30% homology with L-3-hydroxyacyl-CoA dehydrogenase from pig mitochondria and 26% homology with enoyl-CoA hydratase-3-hydroxyacyl-CoA dehydrogenase from rat peroxisomes. It was reported that λ-crystallin has enzymatic functions in tissues other than lens [25]. Recently, we identified several proteins containing D-β-Asp residues from a lens derived cell line [14]. The rate of D-β-Asp depends on the primary amino acid sequence and the steric hindrance of neighboring residues. Therefore, proteins which are susceptible to racemization and isomerization of Asp residues might have highly homologous primary sequence or tertiary structure. Enolase, a glycolytic enzyme that is active as a dimer, and τ-crystallin, a lens protein with three subunits in higher vertebrates, are encoded by the same gene [26,27]. Because enolase functions in the ninth step of the glycolysis pathway, D-β-Asp formation might affect glycolysis. Indeed, racemization and isomerization of an Asp residue within the active site of enolase is likely to abolish the enzyme activity.

In this report, we detected eight D-β-Asp-containing structural proteins and D-β-Asp-containing enolase in rabbit lens. The formation of D-β-Asp residues may be the underlying cause of many diseases, such as the development of cataracts. In fact, this posttranslational modification may explain the clear relationship between aging and some diseased states. A previous study identified the formation of D-β-Asp residues in enolase [14]. In this study, the racemization and isomerization of enolase was induced by IR irradiation.

Despite an incomplete rabbit database, we were able to identify the spots by significant homology to proteins from other species. Our results support the idea that racemization and isomerization of Asp residues in β- and γ-crystallin is caused by aging in mammals. Although many posttranslational modifications are known, racemization involving isomerization has not previously been reported for a lens β-, γ-crystallin. The previous studies indicated that many Asn residues become deamidated in β-crystallins [28,29]. Hanson et al. reported the deamidation at Asn157 in β-B1-crystallin in insoluble proteins of adult lenses [30]. The present study clearly indicates that racemization and isomerization of Asp residues also occurs in a rabbit lens

and increases with IR stress. These modifications are critical to the higher order structure and may disrupt the stability of lens proteins. Further studies are required to elucidate the physiological significance of D-β-Asp-containing crystallin families.

Acknowledgments

We thank Dr. Larry David for his assistance doing our experiments especially with the mass spectrometry. This work was supported, in part, by a research grant from the Ministry of Education, Science, Sports and Culture of Japan.

References

[1] P.M. Helfman, J.L. Bada, Aspartic acid racemization in tooth enamel from living humans, Proc. Natl. Acad. Sci. USA 72 (1975) 2891–2894.
[2] S. Ohtani, T. Yamamoto, M. Sashima, M. Satoh, Age-related changes in the D-aspartic acid content of the cranial bones in senescence-accelerated mice (SAM), Growth Dev. Aging 66 (2002) 35–41.
[3] J.T. Powell, N. Vine, M. Crossman, On the accumulation of D-aspartate in elastin and other proteins of the ageing aorta, Atherosclerosis 97 (1992) 201–208.
[4] A.E. Roher, J.D. Lowenson, S. Clarke, C. Wolkow, R. Wang, R.J. Cotter, I.M. Reardon, H.A. Zurcher-Neely, R.L. Heinrikson, M.J. Ball, et al., Structural alterations in the peptide backbone of beta-amyloid core protein may account for its deposition and stability in Alzheimer's disease, J. Biol. Chem. 268 (1993) 3072–3083.
[5] D. Ingrosso, A.F. Perna, D-amino acids in aging erythrocytes, EXS 85 (1998) 119–141.
[6] P.M. Masters, J.L. Bada, J.S. Zigler Jr., Aspartic acid racemisation in the human lens during ageing and in cataract formation, Nature 268 (1977) 71–73.
[7] N. Fujii, S. Tajima, N. Tanaka, N. Fujimoto, T. Takata, T. Shimo-Oka, The presence of D-β-aspartic acid-containing peptides in elastic fibers of sun-damaged skin: a potent marker for ultraviolet-induced skin aging, Biochem. Biophys. Res. Commun. 294 (2002) 1047–1051.
[8] S.D. Shapiro, S.K. Endicott, M.A. Province, J.A. Pierce, E.J. Campbell, Marked longevity of human lung parenchymal elastic fibers deduced from prevalence of D-aspartate and nuclear weapons-related radiocarbon, J. Clin. Invest. 87 (1991) 1828–1834.
[9] N. Fujii, K. Satoh, K. Harada, Y. Ishibashi, Simultaneous stereoinversion and isomerization at specific aspartic acid residues in α A-crystallin from human lens, J. Biochem. (Tokyo) 116 (1994) 663–669.
[10] N. Fujii, Y. Momose, M. Yamasaki, T. Yamagaki, H. Nakanishi, T. Uemura, M. Takita, N. Ishii, The conformation formed by the domain after alanine-155 induces inversion of aspartic acid-151 in α A-crystallin from aged human lenses, Biochem. Biophys. Res. Commun. 239 (1997) 918–923.
[11] N. Fujii, Y. Ishibashi, K. Satoh, M. Fujino, K. Harada, Simultaneous racemization and isomerization at specific aspartic acid residues in alpha B-crystallin from the aged human lens, Biochim. Biophys. Acta 1204 (1994) 157–163.
[12] N. Fujii, K. Harada, Y. Momose, N. Ishii, M. Akaboshi, D-amino acid formation induced by a chiral field within a human lens protein during aging, Biochem. Biophys. Res. Commun. 263 (1999) 322–326.
[13] N. Fujii, L.J. Takemoto, Y. Momose, S. Matsumoto, K. Hiroki, M. Akaboshi, Formation of four isomers at the asp-151 residue of aged human alphaA-crystallin by natural aging, Biochem. Biophys. Res. Commun. 265 (1999) 746–751.
[14] T. Takata, T. Shimo-Oka, K. Miki, N. Fujii, Characterization of new D-β-aspartate-containing proteins in a lens-derived cell line, Biochem. Biophys. Res. Commun. 334 (2005) 1022–1031.
[15] N. Fujii, Y. Momose, K. Harada, Kinetic study of racemization of aspartyl residues in model peptides of α A-crystallin, Int. J. Pept. Protein Res. 48 (1996) 118–122.
[16] M.M. Bradford, A rapid and sensitive method for the quantitation of microgram quantities of protein utilizing the principle of protein-dye binding, Anal. Biochem. 72 (1976) 248–254.
[17] N. Fujii, T. Shimo-Oka, M. Ogiso, Y. Momose, T. Kodama, M. Kodama, M. Akaboshi, Localization of biologically uncommon D-β-aspartate-containing alphaA-crystallin in human eye lens, Mol. Vis. 6 (2000) 1–5.
[18] D. Yang, N. Fujii, T. Takata, T. Shimo-Oka, S. Tajima, Y. Tanaka, T. Saito, Immunological detection of D-β-aspartate-containing protein in lens-derived cell lines, Mol. Vis. 9 (2003) 200–204.
[19] Y.N. Chirgadze, H.P. Driessen, G. Wright, C. Slingsby, R.E. Hay, P.F. Lindley, Structure of bovine eye lens gammaD (gammaIIIb)-crystallin at 1.95 A, Acta Crystallogr. D. Biol. Crystallogr. 52 (1996) 712–721.
[20] N.H. Lubsen, J.H. Renwick, L.C. Tsui, M.L. Breitman, J.G. Schoenmakers, A locus for a human hereditary cataract is closely linked to the γ-crystallin gene family, Proc. Natl. Acad. Sci. USA 84 (1987) 489–492.
[21] T. Blundell, P. Lindley, L. Miller, D. Moss, C. Slingsby, I. Tickle, B. Turnell, G. Wistow, The molecular structure and stability of the eye lens: x-ray analysis of γ-crystallin II, Nature 289 (1981) 771–777.
[22] E. Heon, M. Priston, D.F. Schorderet, G.D. Billingsley, P.O. Girard, N. Lubsen, F.L. Munier, The γ-crystallins and human cataracts: a puzzle made clearer, Am. J. Hum. Genet. 65 (1999) 1261–1267.
[23] D.A. Stephan, E. Gillanders, D. Vanderveen, D. Freas-Lutz, G. Wistow, A.D. Baxevanis, C.M. Robbins, A. VanAuken, M.I. Quesenberry, J. Bailey-Wilson, S.H. Juo, J.M. Trent, L. Smith, M.J. Brownstein, Progressive juvenile-onset punctate cataracts caused by mutation of the gammaD-crystallin gene, Proc. Natl. Acad. Sci. USA 96 (1999) 1008–1012.
[24] R.S. Smith, N.L. Hawes, B. Chang, T.H. Roderick, E.C. Akeson, J.R. Heckenlively, X. Gong, X. Wang, M.T. Davisson, Lop12, a mutation in mouse Crygd causing lens opacity similar to human Coppock cataract, Genomics 63 (2000) 314–320.
[25] J.W. Mulders, W. Hendriks, W.M. Blankesteijn, H. Bloemendal, W.W. de Jong, Lambda-crystallin, a major rabbit lens protein, is related to hydroxyacyl-coenzyme A dehydrogenases, J. Biol. Chem. 263 (1988) 15462–15466.
[26] C.E. Zomzely-Neurath, Nervous-system-specific proteins: 14-3-2 protein, antigen alpha and neuron-specific enolase, Scand. J. Immunol. Suppl. 9 (1982) 1–40.
[27] L. Fletcher, C.C. Rider, C.B. Taylor, E.D. Adamson, B.M. Luke, C.F. Graham, Enolase isoenzymes as markers of differentiation in teratocarcinoma cells and normal tissues of mouse, Dev. Biol. 65 (1978) 462–475.
[28] K.J. Lampi, Z. Ma, S.R. Hanson, M. Azuma, M. Shih, T.R. Shearer, D.L. Smith, J.B. Smith, L.L. David, Age-related changes in human lens crystallins identified by two-dimensional electrophoresis and mass spectrometry, Exp. Eye Res. 67 (1998) 31–43.
[29] Z. Zhang, D.L. Smith, J.B. Smith, Human β-crystallins modified by backbone cleavage, deamidation and oxidation are prone to associate, Exp. Eye Res. 77 (2003) 259–272.
[30] S.R. Hanson, A. Hasan, D.L. Smith, J.B. Smith, The major in vivo modifications of the human water-insoluble lens crystallins are disulfide bonds, deamidation, methionine oxidation and backbone cleavage, Exp. Eye Res. 71 (2000) 195–207.